Dynamically simulating spruce budworm in eastern Canada and its interactions with wildfire

Hiromitsu Sato, Emeline Chaste, Martin Girardin, Jed Kaplan, Christelle Hély, Jean-Noël Candau, Stephen Mayor

Dynamically simulating spruce budworm in eastern Canada and its interactions with wildfire

Hiromitsu Sato, Emeline Chaste, Martin Girardin, Jed Kaplan, Christelle Hély, Jean-Noël Candau, Stephen Mayor

Dynamically simulating spruce budworm in eastern Canada and its interactions with wildfire

Hiromitsu Sato [a, 1, *], Emeline Chaste [b, 1], Martin P. Girardin [c], Jed O. Kaplan [d], Christelle Hély [e, f, g], Jean-Noel Candau [h], Stephen J. Mayor [a]

[a] Ontario Forest Research Institute, Ministry of Natural Resources and Forestry, Sault Ste. Marie, ON, Canada
[b] Eco&Sols, Université de Montpellier, Cirad, Inra, IRD, Montpellier SupAgro, Montpellier, France
[c] Canadian Forest Service, Laurentian Forestry Centre, Natural Resources Canada, Quebec City, Canada
[d] Department of Earth Sciences, The University of Hong Kong, Hong Kong, China
[e] UMR 5554 CNRS-IRD-Université Montpellier-EPHE, Institut des Sciences de l'Evolution, Montpellier, France
[f] École Pratique des Hautes Etudes, PSL University, Paris, France
[g] Forest Research Institute, Universite du Quebec en Abitibi-Temiscamingue, Rouyn-Noranda, QC, Canada
[h] Natural Resources Canada, Canadian Forest Service, Great Lakes Forestry Centre, Ontario, Sault Ste. Marie, ON, Canada

ABSTRACT

Eastern Spruce Budworm (ESBW) is a major agent of disturbance in Eastern Canada's boreal forests. Outbreaks have historically led to widespread defoliation of its preferred host trees, fir and spruce species, leading to high rates of mortality. This in turn can result in significant economic losses and enhancement of fire potential in the region. Representation of such biotic disturbance has rarely been included in Dynamic Global Vegetation Models (DGVM), which have become essential tools in understanding and predicting forest dynamics in present and future contexts. We present novel representation of host-specific defoliation in a DGVM (LPJ-LMfire), to better represent disturbance regimes in the boreal forest of eastern Canada. Using host foliage density to trigger outbreak, we were able to calibrate and simulate general spatial patterns of defoliation relative to historical aerial sketch map data. Return intervals were thus sensitive to the growth rates of host trees. Modeled return intervals tended to be significantly longer than 30 years, the approximate observed return interval. A factorial experiment was performed on the interactions of ESBW with wildfire, which was found to be slightly enhanced in terms of burned areas after outbreaks due to increased fuel loads. Interactions between ESBW and fire were found to have higher interaction strength in the drier Western region of the boreal forest. Our study demonstrates that biotic disturbance and its interaction with wildfire can be effectively simulated in a DGVM. We show that bottom-up climatic controls are sufficient to drive simulated spatiotemporal patterns of ESBW that can be calibrated to generally match historical observations.

1. Introduction

Dynamic Global Vegetation Models (DGVMs) have proven to be invaluable tools in the large-scale simulation of terrestrial ecosystems, operating effectively in diverse contexts ranging from climate science to palaeoecology (Sato et al., 2021; Koch and Kaplan, 2022). DGVMs are now well-established tools for estimating the impacts of climate change on terrestrial ecosystems and resultant biogeochemical implications (Pavlick et al., 2013; Maréchaux et al., 2021). However, there is a need to improve process representations in DGVMs to better address questions in ecosystem management, restoration, and climate change mitigation and adaptation, which are generally approached at the regional scale. Among the most important of these adaptations include inclusion of regionally specific vegetation at higher taxonomic resolutions and effective representation of critical disturbance regimes (Kautz et al., 2017).

Fire has long been the principal disturbance agent represented in DGVMs with an extensive history of model development and improvement (Thonicke et al., 2001; Li et al., 2012; Hantson et al., 2016, 2020). Fire's frequent occurrence, major role in most terrestrial ecosystems, and that modeling fire is generalizable across ecosystems made it the first priority for implementation into DGVMs (Hantson et al., 2016). Biotic disturbances such as insects and diseases, however, can also have major impacts on forests causing widespread, synchronized defoliation and mortality (McCullough et al., 1998; Pureswaran et al., 2016; Rauchfuss and Ziegler, 2011). Insects and pathogens in turn, can affect successional pathways, species composition, and forest carbon balance significantly (Kurz et al., 2008). Biotic disturbances also may have potent interactions with climate and other sources of disturbance such as

* Corresponding author.
E-mail address: hiromitsu.sato@ontario.ca (H. Sato).
[1] shared lead authorship

management and fire, both natural and anthropogenic (Girard et al., 2008; Canelles et al., 2021). Unlike fire, there have been very few successful efforts to implement a process representation of biotic disturbances in a DGVM despite acknowledgement of its importance (Quillet et al., 2010; Bachelet et al., 2018; Landry et al., 2016; Canelles et al., 2021).

The eastern spruce budworm (ESBW; Choristoneura fumiferana Clem.) is a defoliator native to the boreal and hemiboreal forests of North America that exhibits widespread (-10^5 km^2), periodic outbreaks at approximately 30-year intervals (Boulanger et al., 2012). During major outbreaks, ESBW larvae consume the live foliage of its preferred host tree, balsam fir (Abies balsamea [L.] Mill.), and to a lesser extent, white spruce (Picea glauca [Moench] Voss) and black spruce (Picea mariana Mill.) B.S.P.). After three to ten years of consecutive defoliation by consumption, large-scale synchronized mortality of host trees occurs (Blais 1981; De Grandpré et al. 2019). These budworm-induced mortality events have historically been associated with increased fire risk in the following years (Stock, 1987; James et al., 2017).

Paleoenvironmental proxy studies in the ESBW range has allowed a characterization of the typical frequency and extent of outbreaks on centennial to millennial timescales (Boulanger et al., 2004; Sonia et al., 2011; Navarro et al., 2018). The extent and severity of outbreaks has been hypothesized to have increased since the application of forest management, due to the increase in dense and even-aged balsam fir stands (Blais, 1983; Robert et al., 2012). From an economic perspective, ESBW outbreaks have major destructive effects on potential timber through increased tree mortality and reduced growth rates (MacLean, 2019). During an outbreak (1982–1987), annual losses of wood volume to ESBW are on the order of 10^6 to 10^8 m^3 and accounted for roughly 1.4 times the amount lost to wildfire (Hall and Moody, 1994; Candau and Fleming, 2011). ESBW outbreaks also impact overall forest carbon dynamics through removal of photosynthetically active foliage and dramatically increasing the mortality of host trees. This results in net reductions of carbon uptake and potential shifts from carbon sinks to sources over landscapes of up to 10^5 km^2 (Dymond et al., 2010; Liu et al., 2019). It has also been estimated that ongoing and future climate change may drive more severe outbreaks of ESBW, which would exacerbate current economic and environmental challenges (Candau et al., 2011).

The mechanisms underlying the dynamics of ESBW defoliation are yet to be fully resolved, with the relative importance of bottom-up and top-down controls on outbreak still undetermined. Three theories have emerged to explain the dynamics of ESBW population outbreaks and its synchronized defoliation (Pureswaran et al., 2016). The first of these theories is the silvicultural hypothesis, which posits that forest management practices induced ESBW outbreaks by increasing the amount of large, homogenous balsam fir dominated stands (Miller and Rusnock, 1993). This would then imply that outbreak would be triggered to some degree, by the density of host tree foliage available. An alternative hypothesis, the double, or multiple, equilibria hypothesis, characterizes ESBW populations to have two relatively clear stable states of low and high densities (Morris 1963a, 1963b). The low-density state of ESBW would be maintained by top-down controls such as predation and would be triggered by environmental events such as consecutive warm, dry summers, to transition to the high-density state, while population collapse would result from repeated years of defoliation depleting host foliage. Finally, the oscillatory hypothesis argues that predation, such as by parasitoids, controls levels of ESBW larvae with periodic lapses where ESBW populations can 'escape' this top-down control regardless of external environmental triggers (Royama et al., 2005).

Spatial patterns of ESBW have been closely linked to the density of host foliage, particularly balsam fir, which has shown to have statistical influence over outbreak class (Gray and MacKinnon, 2006). In Ontario, Eastern Canada, spatial analysis of aggregated historical outbreaks suggests the existence of three 'hotspots' that experience frequent defoliation with a radially oriented decrease in activity (Candau et al., 1998). This pattern was hypothesized to be driven by a diffusive decrease in environmental conditions optimal for outbreak, which include a decreasing density of host species. These hotspots exist within a longitudinally-oriented belt in the southern boreal region where patterns of defoliation are roughly correlated with the density of fir biomass (Fig. 1). The southern boundary of this belt, where outbreak frequency is low, has also been found to be correlated with low abundance of host trees (Candau and Fleming, 2005). However, it is likely that the compositional changes associated with climate change may shift host abundances in the future (Pureswaran et al. 2016).

Interactions between ESBW and fire have also long been a topic of interest, given their roles as the two most prominent sources of disturbance in the boreal forests of Eastern Canada. Widespread, synchronized defoliation has been theorized to increase fire potential, starting with qualitative observations that ESBW defoliation preceded large fires (Stocks and Walker, 1973; Navarro et al., 2018). The experimental

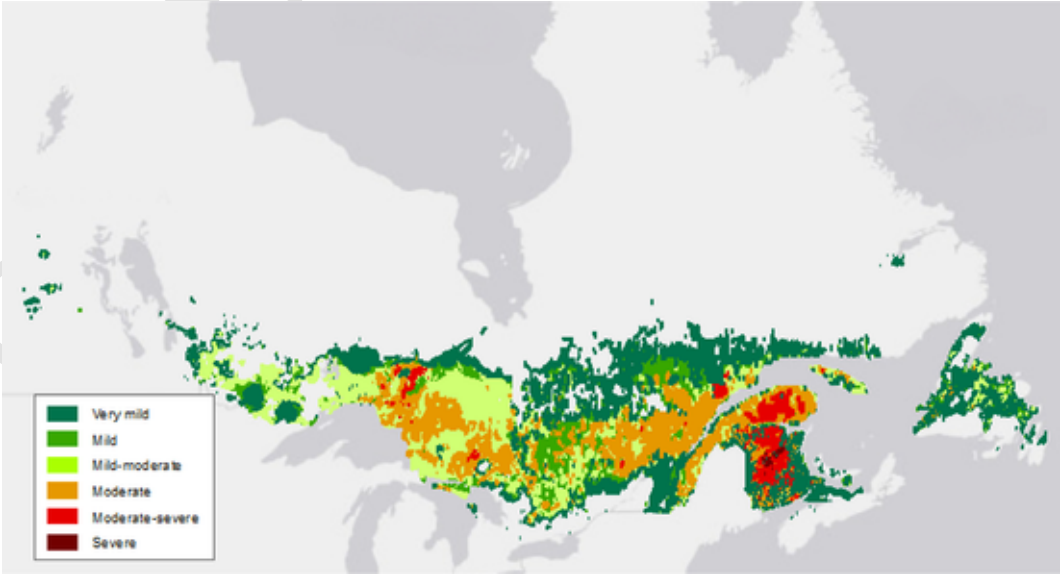

Fig. 1. Cumulative annual defoliation in terms of percent of defoliated areas from 1941 - 1998 expressed in terms of severity classes. Figure adjusted from Girardin et al. (2016) and data originally from Gray and MacKinnon (2006).

burns studied by Stocks (1987) showed high fire intensity and size after ESBW defoliation, though could not provide data to measure the degree of enhancement relative to a control. Modeling studies using historical data have yielded mixed results on the subject, showing nuanced relationships between ESBW defoliation, composition, and fire as opposed to a clear enhancement signal (Sturtevant et al., 2012; James et al., 2011, 2017). From a spatial perspective, interactions between ESBW and fire have been found to be bounded by prevalence of host species to the north, hardwoods in the south, and moisture in the west (Candau et al., 2018). Until now, the specific mechanisms of interaction have yet to be explored using process representations in a dynamic vegetation model that can run over large areas.

In this study, we developed a process representation of ESBW dynamics in the LPJ-LMfire DGVM (Pfeiffer et al., 2013; Chaste et al., 2018). We test how bottom-up controls can determine spatial and temporal patterns of defoliation, as well as the influence of ESBW-driven mortality on wildfire. Outbreaks are triggered by the density of preferred host foliage (Abies) in our simulations. To our knowledge, this is the first attempt at introducing a mechanism to trigger insect outbreak within a DGVM, though others have studied biophysical and biogeochemical implications of defoliation using the IBIS DGVM model (Landry et al., 2016).

We simulate the effects of ESBW on the boreal forests of Eastern Canada over the period 1901–2012 using four representative tree genera (Abies, Pinus, Picea, and Populus). The benefit of using a DGVM in this context is that it effectively simulates a major component of the ESBW ecology: forest dynamics, as the productivity, density, and distribution of host trees is largely determined by environmental conditions and competition. While it may be difficult to currently simulate the entire ecology of ESBW, progress can be made by first simulating independent aspects of their behavior and their impacts on forests, as we approach in this study. LPJ-LMfire is also equipped with a sophisticated fire module, which is capable of simulating the essential aspects of forest fires including fuel dynamics, ignition, and spread. This presents a convenient opportunity to investigate interactions between ESBW defoliation and wildfire to resolve existing uncertainties on the subject.

2. Methods

2.1. Study region and input data

In our study, we focus on the boreal forests of Eastern Canada, where ESBW defoliation is a major source of disturbance. Our study area is approximately 2.9 million km^2, extending from Manitoba to Newfoundland (102–53°W; 46–65°N). The dominant conifers in the region include black and white spruce, balsam fir, jack pine (Pinus banksiana (Lamb.)), and white pine (Pinus strobus L.). Major broadleaf deciduous trees are trembling aspen (Populus tremuloides Michx.), balsam poplar (Populus balsamifera L. (BP)) white birch (Betula papyrifera Marsh.), and yellow birch (Betula alleghaniensis Britt.).

Datasets used to drive our model were prepared as in Chaste et al. (2018). Except for lightning flashes, climate inputs for our experiments on Eastern Canada span from 1901 - 2012 and were generated by BioSIM software from Environment Canada's historical climate database at a 10 × 10 km resolution (Environment Canada, 2013). Lightning flashes, in units of number of cloud-to-ground strikes per day per km^2, were reconstructed for the period of 1901–2012 using the Canadian Lightning Detection Network data set covering the 1999–2010 period as described in Chaste et al. (2018). Soil texture fractions were derived and interpolated from ISRIC - World Soil Information dataset. Atmospheric CO_2 concentrations for 1901 - 2021 were derived from Pfeiffer et al. (2013) and Keeling et al. (2009), as in Chaste et al. (2018).

2.2. Vegetation model description

LPJ-LMfire is a Dynamic Global Vegetation Model from the Lund Potsdam Jena (LPJ) family of models, used for process-based simulation of terrestrial ecosystems at large spatial scales (Sitch et al., 2003). This model has been modified and adapted to serve several purposes as descendent models, with specific upgrades in fire representation, soil processes, and dispersal (Wania et al., 2010;Pfeiffer et al., 2013;Snell, 2014; Chaste et al., 2018). LPJ-LMfire is driven by climate data (i.e., Monthly means of temperature, diurnal temperature range, precipitation, number of days with precipitation, wind speed, total cloud cover percentage and lightning flashes) in tandem with soil, some environmental constraints (water fraction, elevation, and slope) and CO_2 masks (Fig. 2). Outputs include variables characterizing terrestrial vegetation ranging from compositional and structural (e.g., Species, height, canopy density, biomass) to biogeochemical (e.g., carbon uptake, soil carbon, carbon emissions from fires) aspects. Vegetation cover is generated dynamically from bare ground during a 'spin-up' period of about 1000 years using detrended climate data until carbon pools reach equilibrium, then the climate scenario of interest is applied for the transient stage to simulate the period of interest.

Vegetation is described in terms of Plant Functional Types (PFTs), typically covering a wide range of vegetation groups at the global scale (Sitch et al., 2003). PFTs are defined by ecophysiological and biological parameters characterizing key aspects of plant function such as partitioning of carbon resources, bioclimatic limits, and resistance to stressors such heat, drought and fires. Here we used the Chaste et al. (2018) approach of genera-level PFTs for its more direct applicability to regional management and policy. This is particularly useful in regions with a low overall number of dominant tree species, such as the boreal forests of Eastern Canada. The four genera present in this study are Abies, Picea, Pinus, and Populus, which tend to dominate the forests of our study area, and which are each represented by only a few, and usually dominated by one, species (e.g. Abies balsamea). The four PFTs are assumed to be omnipresent, that is, present in every grid cell if environmentally suitable. PFTs establish, then grow and compete within this cell, which then determines composition and abundance. There is no spread of PFTs between pixels, as each grid cell functions independently. Mortality is triggered by a range of processes, such as heat stress, meteorological events, or negative carbon balance. Photosynthate is allocated to fast (foliage) and slow (wood) pools, which shift to litter as a result of both regular turnover and mortality. The majority of litter carbon returns to the atmosphere and the remainder is incorporated into soil organic matter.

The fire module used in LPJ-LMfire (Pfeiffer et al., 2013) is derived from the SPread and Intensity Fire (SPITFIRE) model (Thornicke et al., 2010). Representations of fire occurrence, behavior, and its impacts on vegetation occur in the module. For the purposes of this study, we neglect human-caused ignitions and agricultural burning and only consider lightning-ignited wildfire. Over 90% of fires in Canada have been driven by lightning and agricultural burning is negligible in eastern boreal Canada (Coogan et al., 2021). The probability of wildfire occurring by ignition from lightning is dependent on the amount of available fuel and fuel moisture tracked with the Fire Danger Index (FDI). Lightning occurrence was estimated using the Canadian Lightning Detection Network following by Chaste et al. (2018). Fire behavior simulated using the Rothermel equations (Rothermel, 1972), where the rate of spread and fire residence time are functions of fuel moisture and local meteorological conditions. Fire impacts on vegetation including fuel consumption, tree mortality, trace gas emissions, and burned area are then calculated daily and aggregated for annual output. Fires occur independently without spread between grid cells.

Spin up periods were run for 1120 years using a linearly detrended 1901 - 2012 climate data time series repeated ten times, until carbon pools were in equilibrium and wildfire disturbance stabilized. The orig-

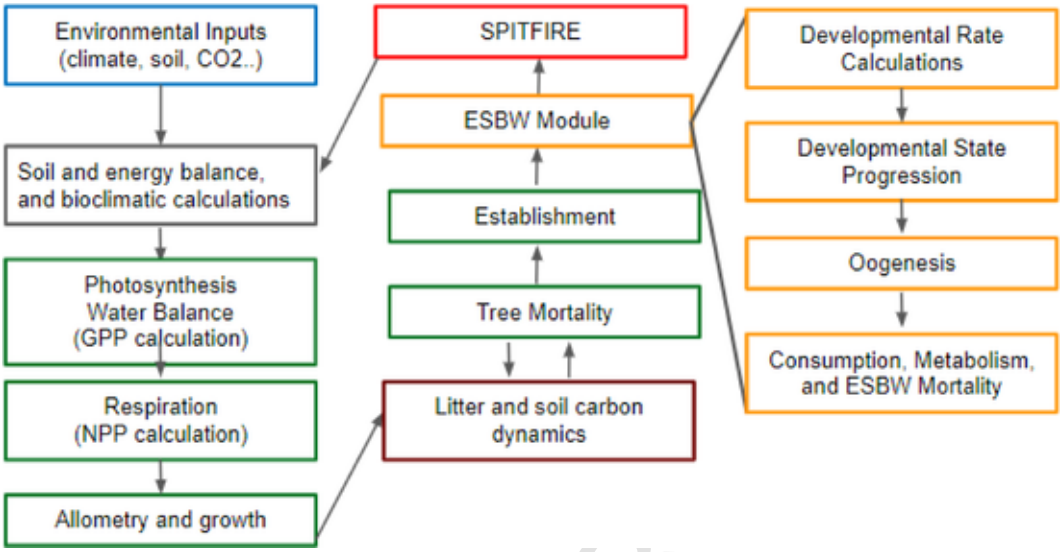

Fig. 2. Conceptual flowchart of LPJ-LMfire including the new Eastern Spruce Budworm (ESBW) module (LPJ-LMfire-ESBW) (modified from Sitch et al. (2003)). Input data, including environmental conditions and PFT-specific parameters (blue), drives biophysical (gray) and tree biological processes (green) including carbon uptake and allocation. Trees are represented by the four typical genera of the Eastern boreal forest (Abies, Picea, Pinus, and Poplar). Mortality due to climate, stress, and fire, or autogenic process such as competition, adds biomass to slow and fast litter pools (brown). The ESBW module and its processes (orange) are activated by a minimum amount of live Abies foliage which initiates host foliage consumption. Fire processes (red) are then calculated with updated litter pools.

inal climate dataset (not detrended) was then run a single time for the transient run, when the ESBW module was activated and tested. For more detail on LPJ-LMfire and its application to Eastern Canada see Pfeiffer et al. (2013), Chaste et al. (2018), and Chaste et al. (2019).

2.3. ESBW module

The ESBW module was designed to simulate the consumption of host foliage over spatial scales larger than 100 km². ESBW is represented in terms of stage development, insect population mass and insect population energy. Larvae development in the module occurs in 10 stages (Egg, L1, L2o, L2, L3, L4, L5, L6, Pupa, Adult) to represent the different steps of development in the spruce budworm life cycle (Miller, 1975). After the metamorphosis process (larvae to moth) during summer, female adults lay eggs over a period of a few days. These eggs hatch in two weeks maximum (L1 stage) and quickly find a suitable place to spin a silken hibernaculum where they molt into the second larval stage and enter an overwintering resting stage (L2o stage) called diapause. No feeding occurs in the L1 stage or during the diapause period so all the energy to survive to the winter is placed in the egg by their mother. During spring, larvae emerge and move to food sites (L2 stage). Once established at feeding sites, over a period of a few weeks larvae develop through four stages of development (L3 to L6 stages) before pupating (Pupa stage). Larvae development occurs by obtaining energy from feeding on needles. Adults emerge in July after metamorphosis (Adult stage) and female moths then lay a new generation of ESBW eggs. In the ESBW module, the state of development at each life cycle stage is represented by a value between 0 and 1, where each cohort begins at 0 and progresses to the next life stage when the state equals 1. Rates of development are calculated through Régnière's process-based development model (Régnière, 1982; Régnière et al., 2012), where rate parameters differ based on sex and life stage and are coupled to climate through temperature dependence (table S1). The rate of development for the L1 stage is represented by Eq. (1), while the adult stage is modeled by Eq. (2), and all other stages are modeled by Eq. (3). Insect masses were derived from two sources: Leonard and Koller (1981) for stages 4–6, pupa and adult, while we used Régnière and You (1991) for stages 2 and 3 (table S2). Developmental parameters were taken from Régnière et al. (2012), which were modified from Régnière (1982, 1983, 1987, 1990) with L1 values taken from Han et al. (2000) and reported in supplementary Table 1.

$$\begin{aligned} &if\ T \geq T_b \left\{ rate(T) \right. \\ &\quad = \beta_1 \exp\left[-0.5 \left(\frac{r-\beta_2}{\beta_3} \right)^2 \right] \Bigg\} rate(T) \\ &\quad = 0\ otherwise \end{aligned} \tag{1}$$

$$if\ T_b \leq T \leq T_m$$

$$\left\{ rate(T) = \beta_1 \left[\frac{1}{1+e^{\beta_2-\beta_3\tau}} - e^{\frac{r-1}{\beta_3}} \right] where\ \tau = \frac{T-T_b}{T_m-T_b} \right\} rate(T) = 0\ otherw$$

$$\left\{ rat\,e(T) = \frac{1}{\beta_1 + \beta_2\tau + \beta_3\tau^2} \times where\ \tau = \min\left[\max(T, T_b), T_m \right] \right\} \tag{3}$$

ESBW larvae progress through their life stages internally at a daily time step, though the model produces output at annual intervals (annual foliage consumption, L2O mass, insect energy). Development of larvae only occurs when daily temperatures are between 2.5 °C and 32 °C. Oogenesis and oviposition are estimated by calculating the total number of females and assuming that each has a potential 200 eggs to lay, scaled by an increasing linear function of air temperature (Régnière, 1983). Oogenesis is only possible under three conditions: (1) presence of adult female insects, (2) adult female insects are mature (state of development is > 0.0666), and (3) temperature is between 10 and 25 °C. L2o larvae can survive winter temperatures greater than −10 °C while consuming energy from the egg state (Fig. S1). The value of 0.06 corresponds roughly to one day for a female adult's life stage progression. Well-fed, mated females do not lay eggs in the first 24 h after emergence, laying a third to a half of their eggs during their second day.

2.3.1. Modeling bottom-up controls on ESBW

In our study, we assume that a minimum amount of Abies leaf biomass is required to trigger the initial presence of ESBW larvae. Under influence of the silvicultural hypothesis, we selected Abies foliage density to be the sole determinant of larval colonization. This is a simplification, and some combination of host tree foliar density could feasibly be used to trigger initial colonization given comparable preference for Picea Glauca and its importance in the western margins of its distribution. Thus, Picea foliage does not contribute to colonization of ESBW in our study though it is consumed along with Abies during defoliation events. Foliar biomass is a function of both host tree density and tree age and size (Akalusi and Bourque, 2021;Temesgen and Weiskittel, 2006). We hypothesize that there is an approximate minimum amount of foliage required to support an outbreak, which is an assumption of the double-equilibria hypothesis. This is a practical simplification of a density-dependent process that is sufficient for our study.

From here, we refer to the minimum value of fir foliage that triggers colonization as the 'Leaf Mass Threshold' (LMT). Parasitism and predation on ESBW may also be important controls on ESBW density, particularly at low population densities, but our model simplifies its dynamics and excludes these processes. We likewise exclude anthropogenic control measures of ESBW which aim to limit tree mortality and anthropogenic drivers of tree community composition such as forest harvest and silviculture.

2.3.2. Consumption of foliage

Consumption of host foliage, energy accumulation, and usage are calculated by taking the number of individual larvae within an instar and multiplying it by the rate of consumption as measured in vial-based experiments by Leonard and Koller (1981) (table S3). If temperature is below −10 ˚Celsius, all larvae except for L2o are killed (Régnière, J., and Nealis, V. G., 2019). Though Régnière and Nealis (2019) focused their study on the western spruce budworm, this specific mortality condition was developed with reference to studies on the frost tolerance of ESBW larvae (Han and Bause, 1995). Warm temperature sensitivity is represented by a temperature dependent metabolism function, which accounts for the potential for overwinter starvation (eq. (4)) (Régnière et al., 2012). Life stage progression and consumption is halted if daily temperatures are outside a temperature window of 2.5 to 32 ˚Celsius. Energy is still consumed during these days and mortality occurs if larvae deplete their energy reserves.

$$energyloss = 8.6623e^{-11} * t_{mean}6.5241 \quad (4)$$

The ESBW module interacts with LPJ-LMfire through both direct effects on tree growth and mortality and indirect effect on the probability of fire by increasing fuel loads. Consumption of live foliage from host trees (Abies and Picea) reduces carbon uptake, while foliage and wood from the ESBW killed trees are transferred to the litter pools. The ESBW module runs prior to fire and delivers information on fuel (litter) biomass to the fire model on an annual time step. The size of this timestep is appropriate for this study given that budworm-driven enhancements of fire tend to occur years after mortality due to fuel drying and fuel ladder development (James et al., 2017).

In our initial model simulations, foliage of the host trees was completely consumed by ESBW after two to three simulation years. Field observations show that ESBW defoliation typically takes up to 10 years prior to mortality (Chen et al., 2017). A number of factors could explain this overestimated rate in the model, including: i) lack of bottom-up control on ESBW through parasitism or predation, and ii) idealized food availability. ESBW is also a very wasteful eater, consuming only a fraction of the total quantity of foliage on twigs and branches that die as a result of defoliation. As a result, more foliage is lost than what is actually consumed. ESBW larvae only consume current year foliage whereas in this version of our model, host foliage from any year is available for consumption. This additional restriction would likely extend the time from initial colonization to tree mortality and would be a useful addition to future iterations.

We addressed this inaccuracy in the model by imposing a scaling factor on the rate of foliage consumption. To slow consumption rates to more realistic levels, we multiplied rates by a constant value between 0 and 1 that we refer to as the consumption coefficient. The length of defoliation period showed an inverse relationship with consumption coefficient (cc), with cc = 0.35 inducing an outbreak length of approximately 5–10 years (Fig. S3). This method, though simple, sufficed for our purposes given that our study was focused primarily on the impacts of ESBW outbreak on forests over longer timescales.

The return interval showed strong sensitivity to LMT variation (Figs. 6 and 7). In our model, unimpeded consumption will lead to complete defoliation and subsequent complete mortality, which repeats as cover regenerates and foliar density reaches the LMT. In reality, there is often an understory of suppressed host trees that is less affected by ESBW outbreak that will resume growth after opening of the stand canopy (Lavoie et al., 2021). Our initial tests that allowed for complete mortality of host trees resulted in return intervals up to an order of magnitude larger than observed values. To remedy the slow growth rates and reflect residual host trees surviving after outbreaks, we allowed a small amount of foliage to survive post-outbreak. Mortality was then defined to a set amount in accordance with past studies. Slow and fast litter from the killed trees were then allocated to total pools accordingly. MacLean (1980) presented average post-outbreak mortality for mature (85%) and immature balsam fir (42%) stands. Spruce stands were found to have significantly lower average mortality for both mature (36%) and immature (13%) cases. Given that LPJ-LMfire does not have stand age incorporated, an average of these two values was taken to estimate the modeled mortality, which was 64% for fir and 25% for spruce. Application of this method yielded significantly faster regrowth post-outbreak, but still slower than observed values.

2.4. Modeling experiments

Three modeling experiments were performed to assess spatial and temporal patterns of ESBW outbreaks, and their interactions with fire. First, we tested the sensitivity of long-term defoliation to a range of LMT values to generate a set of spatial patterns of ESBW outbreaks comparable to observations in eastern Canada, where ESBW is monitored annually by field and aerial surveys. LMT was tested over a range of values, resulting in a distinct set of defoliation patterns that could be compared and calibrated to those of Gray and MacKinnon (2006). To test the response of outbreak return interval against the LMT, we ran a sensitivity test of fir foliage density over time (including frequency of foliar collapse) to LMT. Simulations were run over a range of LMT values in a smaller region on the Ontario-Quebec border where an outbreak occurred in all runs. Return intervals, defined as the time period between two consecutive ESBW defoliation events, were averaged over three consecutive outbreaks in transient runs from ten cells from regions defoliated in all runs (intersection of all runs). In the case of return intervals over 100 years, outbreaks during spin-up immediately prior to the transient stage were taken into consideration.

To test interactions between fire and ESBW defoliation on fir foliage density, we performed a factorial experiment with four scenarios: a) control scenario without any natural disturbances b) fire only c) ESBW only and d) fire and ESBW. To assess the effects of ESBW integration on burned area fraction, gross primary productivity, slow fuel, and carbon emissions variables from fire-only runs were simply subtracted from the fire-and-ESBW runs.

2.5. Model evaluation

Consolidated aerial sketch map data on ESBW defoliation in Canada from 1941 to 1998 were sourced from Gray and MacKinnon (2006)

through personal communication. We developed a ground-truth dataset for model evaluation by creating a binary categorization of the aerial sketch map data. Though Gray and MacKinnon's (2006) contained categorical outbreak classes, we chose to convert both model and aerial sketch map data to binary classification given the qualitative nature of ASM outbreak classes. All classifications of outbreak, ranging from very mild, mild, mild-moderate, moderate, moderate-severe, severe, to very severe, were interpreted as outbreak occurrence indications. Shapefiles of outbreak classes were reclassified to the binary categories of 'defoliation present' and 'defoliation absent' and rasterized in alignment with model output in ArcGIS 10.7.1.

To quantify agreement between model output and aerial sketch-map based measurements of defoliation, we computed the Jaccard coefficient for each scenario relative to data by Gray and MacKinnon (2006). The Jaccard coefficient is a simple metric of similarity between two sets of data, calculated by dividing the intersection (number of grid cells of model-data agree on defoliation presence) by the union (total combined number of grid cells with defoliation by either model or data).

3. Results and discussion

3.1. Spatial patterns of outbreak through host tree density

Defoliation patterns showed strong sensitivity to LMT variation, with low values of LMT resulting in very broad distributions of defoliation and high values resulting in a narrower, concentrated southern pattern (Fig. 3). A low LMT results in ESBW appearing wherever Abies appears, even at low levels, while at higher thresholds ESBW only populates regions dense in fir. Simulated distributions of cumulative consumption generally match patterns of defoliation as found by Gray and MacKinnon (2006) at the higher end of LMT. The latitudinal belt of ESBW defoliation found by Candau et al. (1998) in Ontario was also present in our simulations across Eastern Canada, particularly at the higher end of LMT values. This belt is where Abies foliage is most dense and thus where environmental conditions are optimal for Abies growth and fitness against other PFTs. This is consistent with findings by Candau and Fleming (2005). This suggests that host tree density may be an important factor in defining the southern boundary of defoliation, which could shift northward under climate change scenarios.

The spatial distribution of frequent outbreaks (hot spots) was generally well simulated: past defoliation in historical aerial sketch maps were co-located with areas of high defoliation in our simulations, though a strip of heavy defoliation was found (Fig. 2) instead of point locations (Candau and Fleming, 2005; Gray and MacKinnon, 2006) . This can be attributed to model overestimation of Abies density in this region, as found by Chaste et al. (2018) evaluation of LPJ-LMfire's model skill in simulating genus-level biomass in Eastern Canada. Note that in their study and ours, LPJ-LMfire simulates potential vegetation based on environmental drivers and does not include the effects of management on composition. Management has been suggested to be the reason underlying low density of host species in corridors separating hotspots and could explain the difference in patterns between our simulations and observation (Candau et al., 1998; Belyea, 1952). Regions of high levels of defoliation in our simulations are generally surrounded by areas of lower levels of defoliation, tapering off to zero. By assuming outbreaks to be dependent solely on the density of host foliage, we also see the radially diffusive patterns of outbreak frequency.

An LMT of 30 g/m^2 was found to drive simulations with highest agreement with ASM data, as model-data agreement, assessed using the Jaccard coefficient (Fig. 4a), tended to increase gradually toward an optimal value, with a quick drop off afterward. This best run scored a Jaccard coefficient of 0.45, which is notably higher in agreement than a random model (Jaccard coefficient = 0.20, see Fig. 4a). Total modeled values of live foliar biomass for Picea, Pinus, and Populus PFTs are at the lower end of empirical estimates but within an order of magnitude of measured average oven dry foliage biomass from mixed coniferous deciduous forest (Tadaki, 1966). Fig. 5 (a,b,c) shows the binary presence/absence re-classification of model output and Gray and MacKinnon's data set and the intersection of these two data sets of the model parameter set that showed highest agreement with data.

The complement between model output and ASM data was also calculated for the run of highest agreement (Fig. 5d). Regions of disagreement include model simulations showing relatively higher outbreak severity in eastern Newfoundland and Labrador and Nova Scotia. In the case of Newfoundland and Labrador, this overestimate can be traced to LPJ-LMfire's tendency to significantly overestimate Abies biomass in the eastern region, likely due to overestimates of soil fertility (Chaste et al., 2018). Northern regions of Quebec also show low levels of defoliation even at the higher end of LMT, which are not observed in Gray and MacKinnon's (2006) analysis but appear within the northern boundaries of ESBW presence as found by Régnière et al. (2012). Thus, lack of survey data rather than defoliation may underlie model-data disagreement particularly due to the northern limit of surveys in Quebec and for all of Nova Scotia (Gray, 2013).

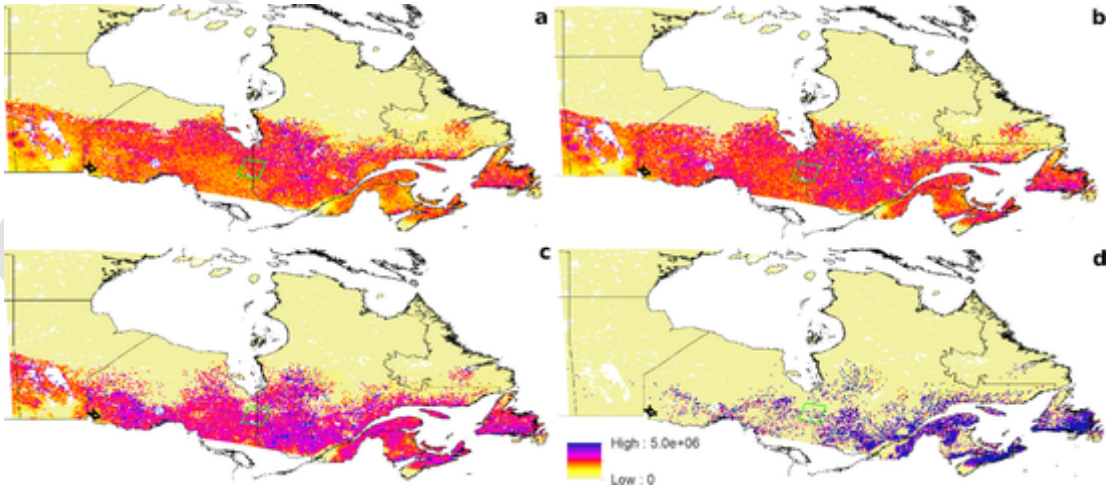

Fig. 3. Mean simulated defoliation over a 100-year period across Eastern Canada for a range of values of Leaf Mass Threshold (a) 5 g/m^2 b) 15 g/m^2 c) 25 g/m^2 d) 35 g/m^2). The full set of runs are shown in fig. S2. The smaller box in green shows the sample region where temporal patterns were taken from. Darker colours indicate high levels of fir foliage were defoliated while yellow indicates low levels.

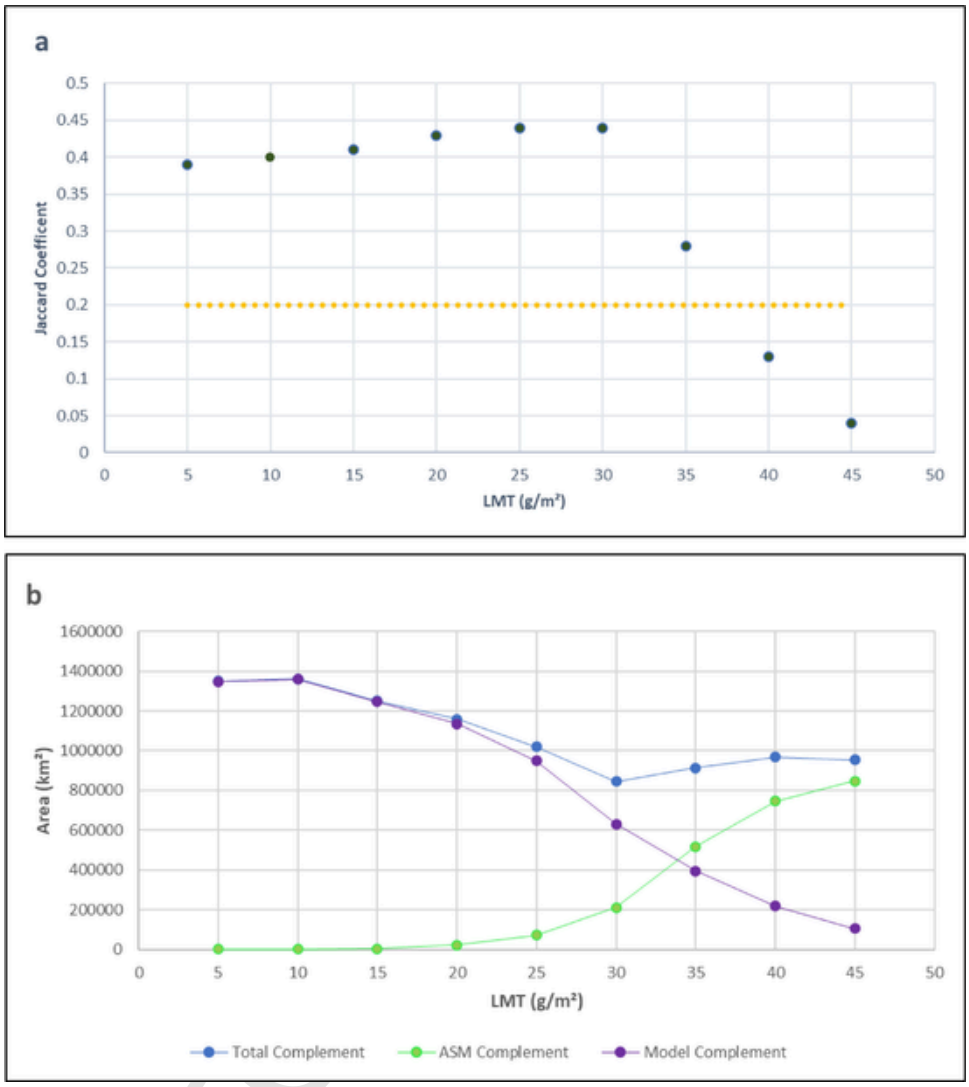

Fig. 4. (a) Jaccard coefficient representing model-data agreement between binary reclassification of ASM data and model output. The orange dotted line shows the Jaccard coefficient corresponding to the random model.
b) Total amount of area where model and data disagree (blue) decomposed into area defoliated as observed by ASM that was not simulated by model (i.e. ASM complement/omission error in green) and area defoliated as simulated by model that was not observed by ASM data (i.e. model complement or commission errors in purple).

3.2. Temporal patterns of outbreaks (return interval)

Fig. 7 shows return interval sensitivity to LMT for both intermediate and immature mortality values. Based on model assumptions, the frequency of outbreak has an inverse relation to the level of mortality in stands in our model. Assuming all stands to have low mortality as prescribed by MacLean's (1980) values for immature stands resulted in the fastest and most realistic return intervals. However, the assumption for all stands to be immature and mortality to be this low is unrealistic, suggesting that selective regrowth may be too slow in the model.

Triggering outbreaks by host foliage density produced roughly regular intervals based on the regeneration rates of host foliage and the value of the threshold parameter (LMT), as prescribed by versions of the silvicultural hypothesis (Pureswaran et al., 2016). The degree of mortality also showed significant influence on the length of return intervals. Our results are roughly in agreement with regeneration-based theories of ESBW outbreak. However, this representation would be inconsistent with theories of outbreak that posit external influences such as predation and parasitism to be critical controls of defoliation onset and cessation (Johns et al., 2019; Régnière et al., 2019).

The value of LMT that resulted in a return interval closest to observation was still much lower than the value that produced best spatial pattern agreement. However, our simulated defoliation patterns were based on potential fir distributions and neglected the effects of management and their effects on fir density. Furthermore, lack of survey data where ESBW occurred, such as in northern Quebec, may have resulted in increased commission error. Thus, the LMT that best fits actual outbreak patterns could potentially be significantly lower.

3.3. Interactions between ESBW and wildfire

The ESBW module progressively decreased the amount of fir foliage during outbreak with subsequent regrowth (Fig. 8c and d). The results of our factorial experiment also showed that fire tended to decrease the overall volume of fir foliage by up to roughly half of its control values. Regeneration of fir foliage was also slower when fire was present (Fig. 8b and d). ESBW presence triggered clear, but small increases in burned fraction after defoliation events relative to control (Fig. 9a). As living leaf mass from host trees decreases, carbon uptake decreases while respiration values remain roughly constant resulting in lowered net uptake

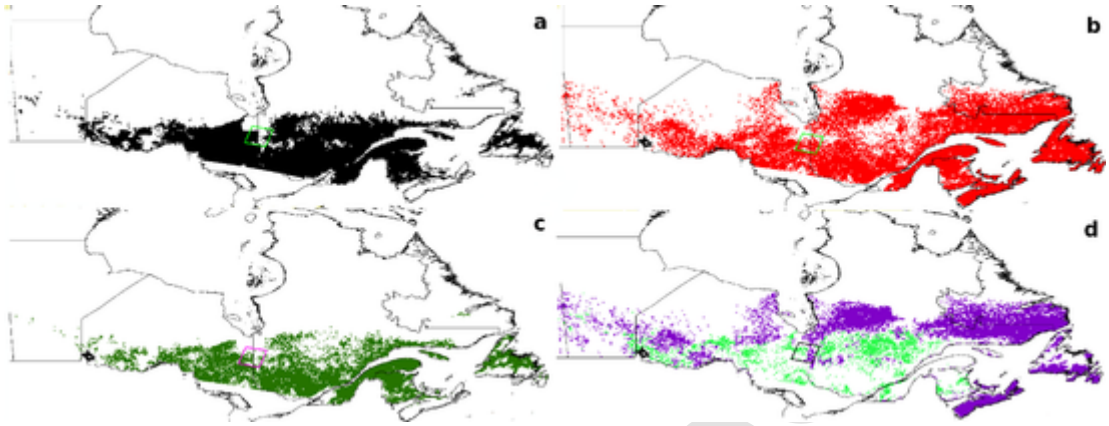

Fig. 5. Binary reclassification based on the presence or absence of defoliation for a) Gray and MacKinnon's data (2006) and b) model output for 30 g/m^2, their c) agreement (intersection) and d) disagreement (complements). For 4d, purple represents regions where the model simulates ESBW defoliation not observed by ASM (i.e. commission errors, while light green represents regions where ASM showed ESBW defoliation that was not simulated by the model (i.e. omission errors).

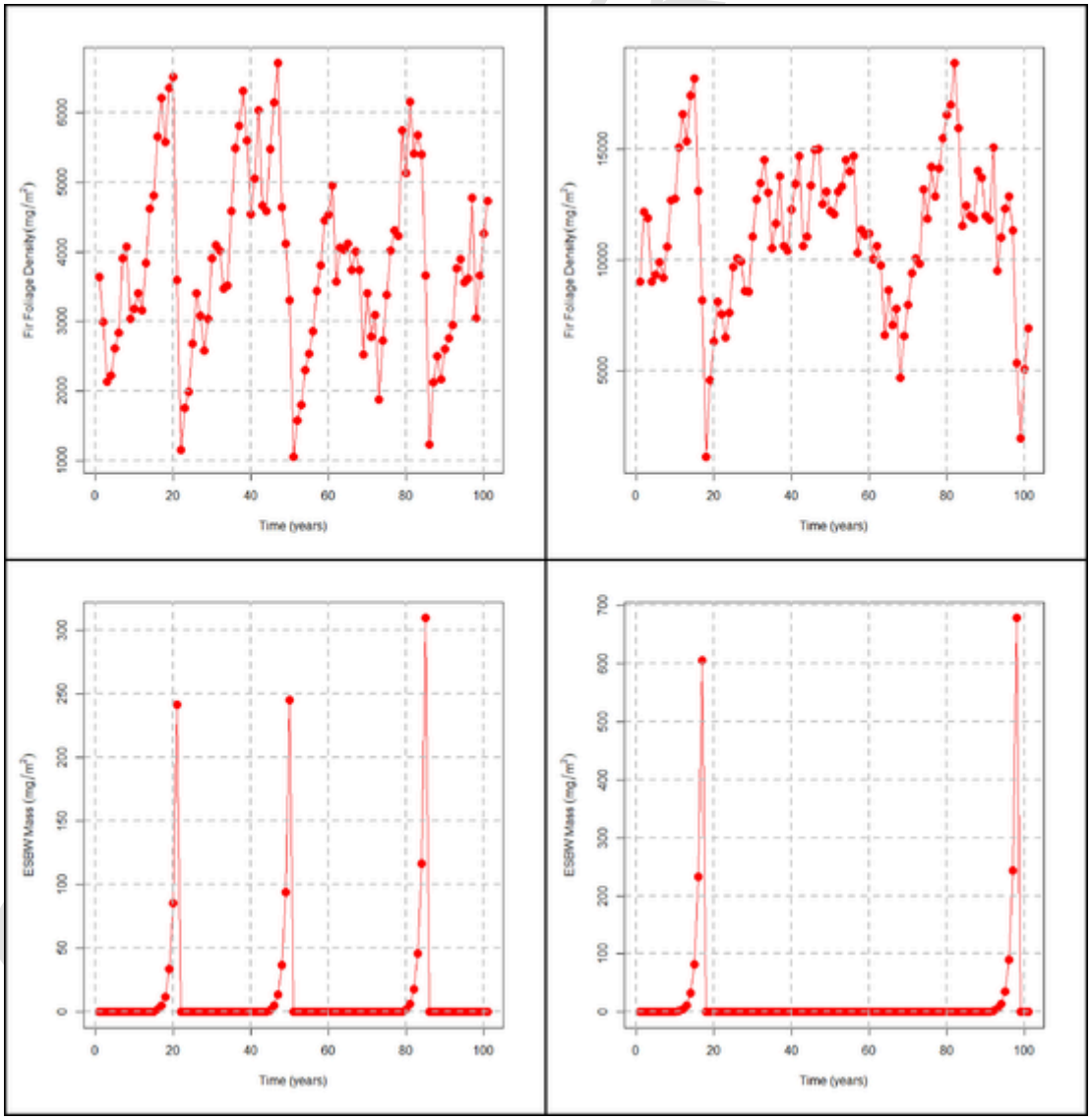

Fig. 6. Sample within-pixel time series for fir foliar biomass and ESBW mass for LMT values of 5 g/m2 (left) and 15 g/m2 (right).

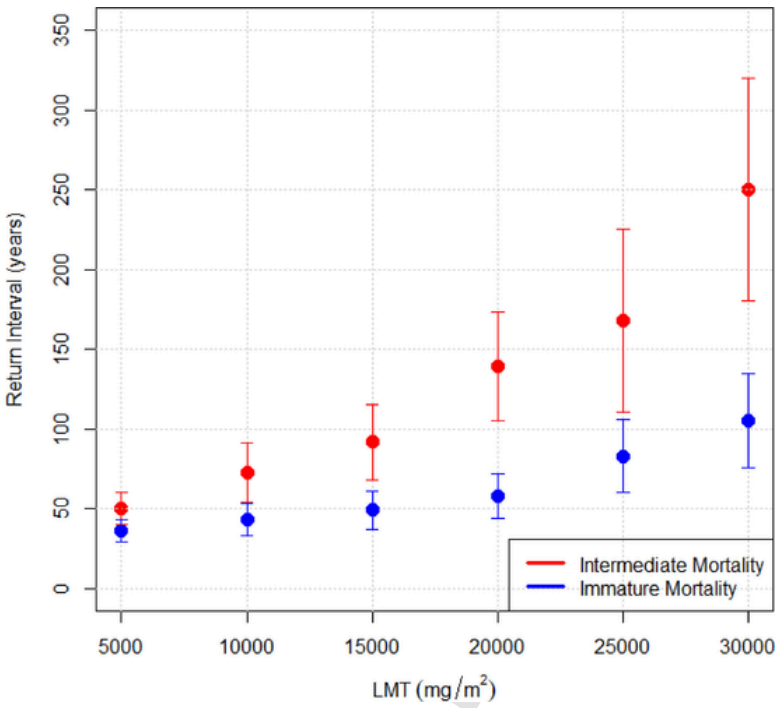

Fig. 7. The sensitivity of average return intervals to LMT over a range of LMT values for intermediate and immature mortality rates with error bars for their respective standard deviation.

(Fig. 9d). After defoliation, there is a small, sustained increase in burned area (<1.8%) ((Fig. 9a). This coincides with a sudden rise in slow fuel caused by mortality of host trees (Fig. 9b). Increases in dry fuel leads to an increase in the rate of spread (ROS). Our simulations show that defoliation-induced mortality leads to an increase in fuel load and an increased likelihood of ignition and larger fires. This initial increase in burned area relative to control is followed by a decrease, due to depletion of fuel. Carbon emissions from fire are also enhanced due to ESBW in proportion to burned area.

At 'intermediate mortality' rates, ESBW defoliation generated an average of 890 g/m^2 of burned fuel from killed host trees, which resulted in at least small increases in burned area (Fig. 9a). In certain grid cells, one may see larger enhancements of burned area fraction in a single fire when there is a large amount of dead fuel caused by defoliation and fire spreads into living biomass (9a). When averaged over the entire region, these effects are attenuated to an average of less than 1%. When averaged over time, the overall amount of burned area of sites with and without ESBW is small even for cells with strong pulses of enhancements in burned area.

To assess the larger spatial variation of the ESBW-fire interaction, average increases in burned area after defoliation driven mortality were plotted across eastern Canada. Interactions were found to be stronger in the west relative to the east (Fig. 10). Drier climate in the western part of the study area may explain, in part, stronger interactions relative to the eastern part of the boreal region studied. Extreme summer temperatures in Ontario may also contribute to higher interactions relative to the Maritimes. In terms of moisture representation within LPJ-LMfire, the probability that a fire will be triggered by lightning is represented by the dependence of ignition efficiency on Fire Danger Index (FDI), which in turn is a function of soil moisture. Moisture of extinction is also represented in the FDI, which is the upper bound value above which fire will not spread. This is consistent with analysis that suggests the sensitivity of fire regimes to be higher in drier environments with a shorter fire cycle (James et al., 2017). Fleming et al. (2002) also found a general pattern of decreasing interaction strength from the drier climate of the west to the wetter east, suggesting that drier climates would lead to slower decomposition, and could extend the season of heightened fire potential and likelihood of successful ignition.

Our simulation of ESBW-fire interactions agree with previous modeling studies, and importantly, the experimental results of Stocks' (1987) fire burn experiments, and theorized observed impacts of ESBW defoliation on forest carbon dynamics (Fleming et al., 2002). It is difficult to compare our results with Stocks' work given the lack of control cases in past burn experiments to demonstrate how ESBW may lead to a relative enhancement of burnt area. The positive but small enhancement of fire by ESBW-defoliation modeled in our study could explain the subtle or null effects of ESBW on fire risk found by James et al. (2011) and Sturtevant et al. (2012). In these cases, analyses at larger scales in which small pulses of enhancement may be 'washed out' over larger spatiotemporal scales. That is, positive feedback from defoliation on burning may be largely canceled out by subsequent negative feedback averaged over longer timescales due to depleted fuel loads. Similarly, post-fire stands in boreal forest have been found less likely to burn due to reduced biomass and slow regrowth (Parisien et al., 2020). In reality, the interactions between fire and ESBW are likely to be highly context dependent, with wind and soil conditions likely playing important roles.

It should be noted that there is no interaction between grid cells in LPJ-LMfire, so each disturbance (i.e., fire and ESBW) does not spread between cells. This is very likely to underestimate the importance of single, large fire events that could rapidly grow or join. Additionally in our model, the absence of fire leads to higher density and growth rates of fir foliage. Assuming that fir foliage density triggers outbreaks, this could lead to both shorter return intervals and broader outbreaks. This is consistent with silvicultural hypotheses that postulates that management, including fire suppression, could promote the occurrence of ESBW outbreak by promoting Abies. This aspect could be further explored in future studies, given its consistency with Blais (1983) and its relevance to management practices.

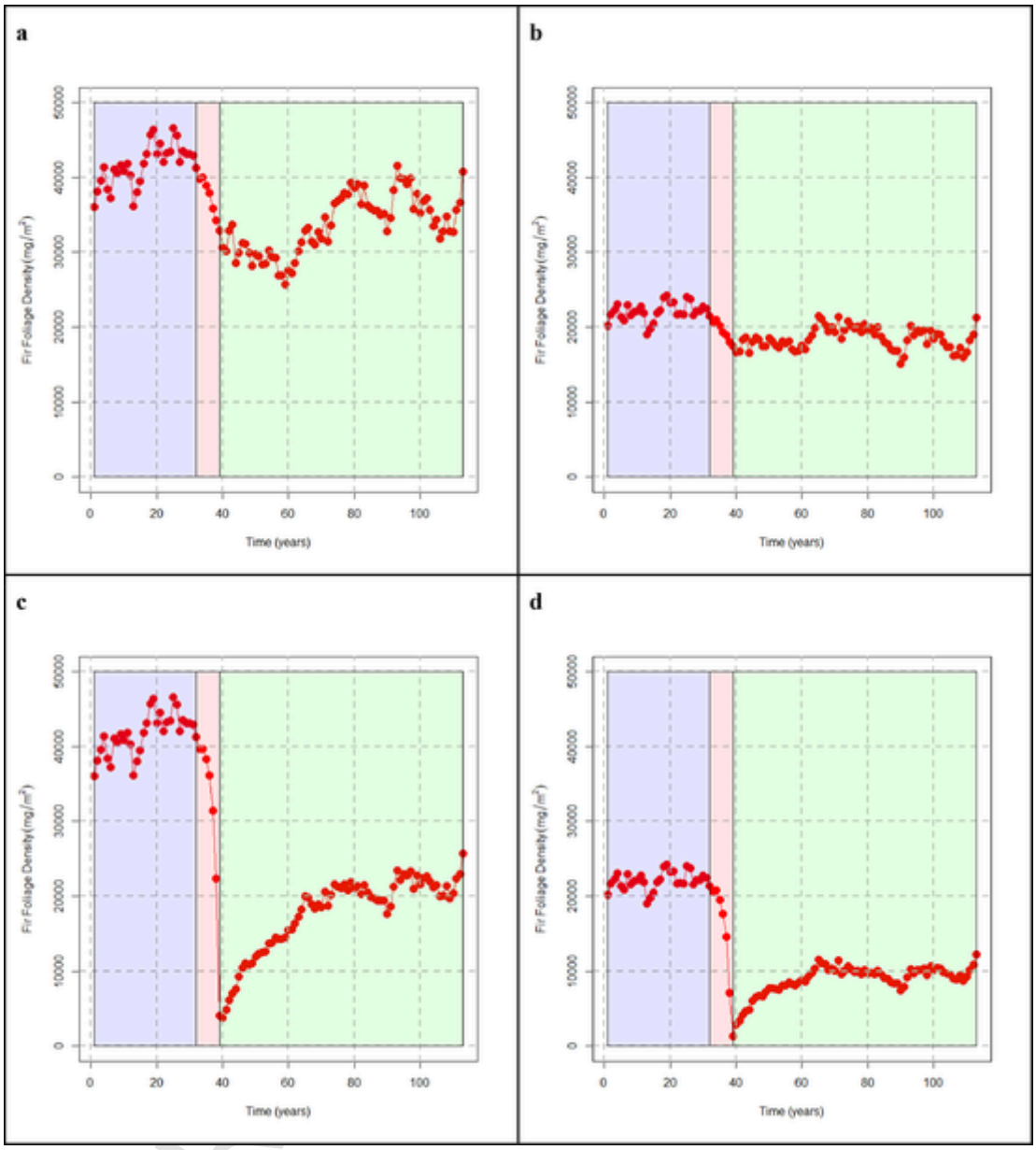

Fig. 8. Fir foliage density for a) control b) fire-only c) ESBW-only and d) fire-and-ESBW. Blue shading indicates time before outbreak, red shading indicates time during defoliation, and green shading represents time after defoliation.

4. Concluding remarks

Our study shows that the assumption that ESBW outbreak and defoliation is triggered by the density of fir foliage has a number of consequences. Linking defoliation to modeled Abies density produced results in general agreement with consolidated aerial-based observations of ESBW defoliation, with model-data agreement peaking at an intermediate value within the tested range of threshold values. It is noteworthy that our simulation generated dynamic distributions of Abies and Picea from bare ground, using only ecophysiological parametrizations of each PFT reacting to environmental drivers. Competition between these PFTs, mediated by their growth parameters, determined stands (i.e. grid cells) composition and density across time and space. Thus, the ability to simulate spatial patterns of defoliation is highly contingent on successful simulation of Abies. It is natural that to simulate the large-scale patterns of the parasite, one must first successfully simulate the patterns of the host.

Given the ability to estimate the general patterns of ESBW defoliation, including belt, zone, and hotspot type spatial patterns, we posit that our methods may be sufficient as a first-order approximation of spruce budworm-fir dynamics. While parasitism, predation, and dispersal are likely important controls of outbreak dynamics, this method would at least conceivably give an upper bound on the extent of outbreak size. Host foliage biomass may not be the sole trigger of outbreak, but it is likely a requisite condition as fuel is to fire. This will be even more important when projecting out future patterns of ESBW defoliation, given the potentially major climate change driven changes in tree composition (Chaste et al., 2019). Moreover, indirect and non-climatic processes such as CO_2 fertilization, fire, and interaction between disturbances, will likely play a factor in these shifts. For these reasons, this insect-adapted DGVM version of LPJ-LMfire (LPJ-LMfire-ESBW) could be a powerful tool in forecasting large scale changes in defoliation and discerning underlying mechanisms.

Future work could improve on several aspects to modeling biotic disturbance in a DGVM. First, dispersal is likely necessary to better rep-

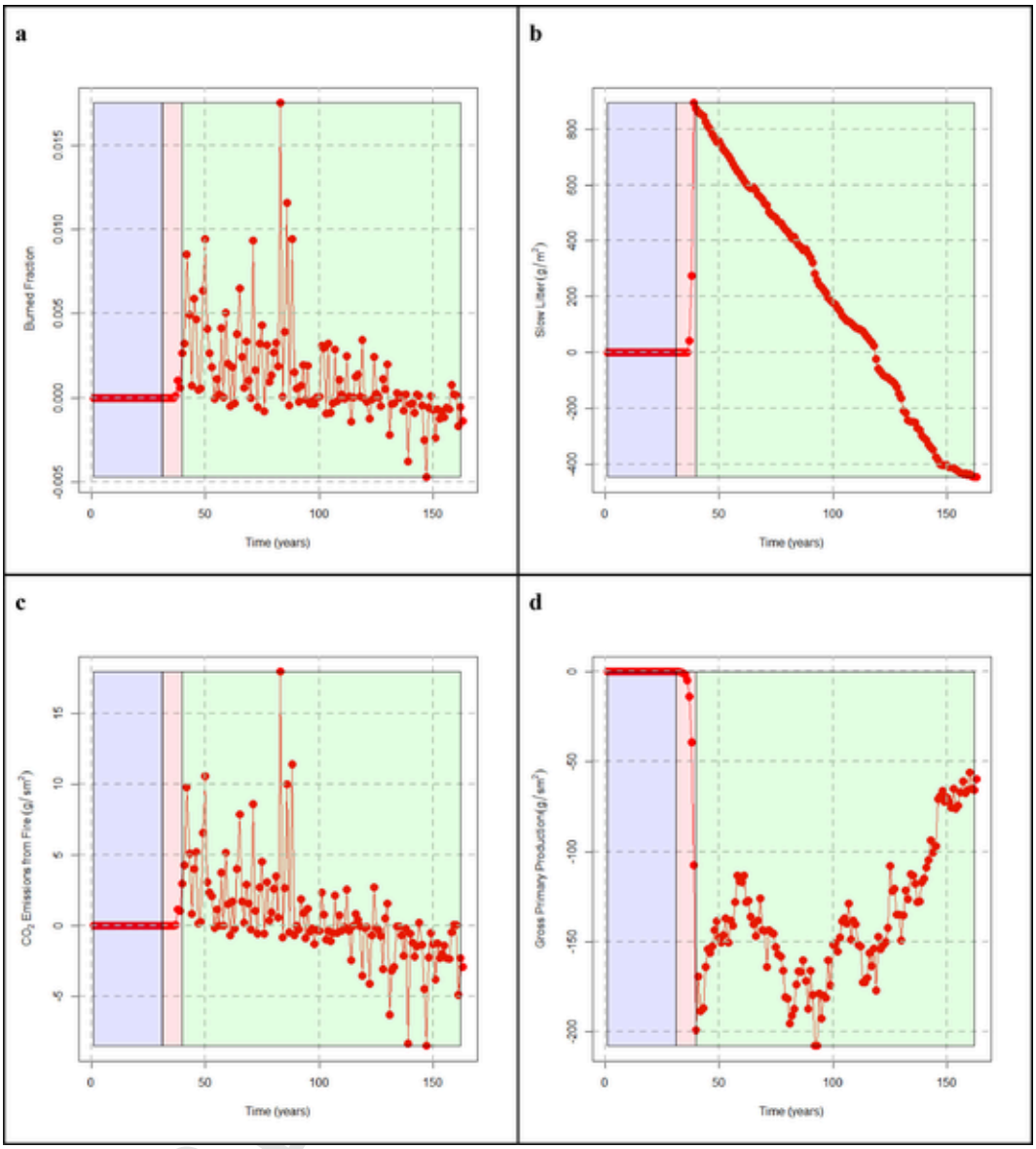

Fig. 9:. Effects of ESBW defoliation averaged over a 10 000 km^2 area on (a) burnt fraction, (b) slow litter (dead trees), (c) fire-driven CO2 emissions, and d) GPP, as derived from our factor separation test. Positive values indicate an increase in the variable due to the influence of defoliation, while negative values indicate a decrease.

resent defoliation dynamics. To integrate dispersal would require inter-cell interactions, which has long been absent in other major forest processes such as fire and seed dispersal. These interactions would likely change results significantly and could improve spatiotemporal dynamics. Second, ESBW is likely controlled not only by foliage availability but also by parasitoids (e.g. Cappuccino et al. 1998, Régnière et al. 2020) and avian predators (e.g. Crawford et al. 1983, Crawford and Jennings 1989, Venier and Holmes 2010). Additionally, a mechanistic approach to host preference could be implemented to account for potential future changes. There has been evidence that changes in phenological synchrony between budbreak of host trees and emergence of L2o diapause phase could alter host preference from balsam fir to black spruce and subsequently, push ESBW distributions northward (Pureswaran et al., 2019). Increasing the number of PFTs to include genera such as Birch and Maple would improve realism in forest regeneration and possibly alter post-fire fuel dynamics, particularly in the Southern boreal where community composition is more diverse. Another avenue to improve upon would be working toward a sufficiently detailed representation of fuel structures and understory vegetation to enable more complete simulation of the delayed positive feedback of defoliation on fire as suggested by Stocks (1987).

Our study was one of the very first attempts at integrating insect-driven defoliation and biotic disturbance within a DGMV. Relative to fire, modeling insect disturbance requires a more specific understanding of the disturbance agent's ecology, physiology, and its relationship to its host or multiple hosts. We suggest this is an opportunity for entomologists, ecologists, and earth systems scientists to work together to better understand the role of biotic disturbances within the context of global change as many insect species affect forests worldwide and in turn the carbon storage trees represent. Here, we opted to investigate ESBW, but the architecture of our model may be transferable to other species, particularly other defoliators, with appropriate revision and reparameterization. For broader scale or global models, researchers may consider broader functional classifications of biotic disturbance agents, such as defoliators, wood boring insects, fungal pathogens, etc.

Using the bottom up controls of host foliage density to trigger initial outbreak, we effectively simulated the spatial patterns of ESBW and produced regular return intervals. We suggest that these results may

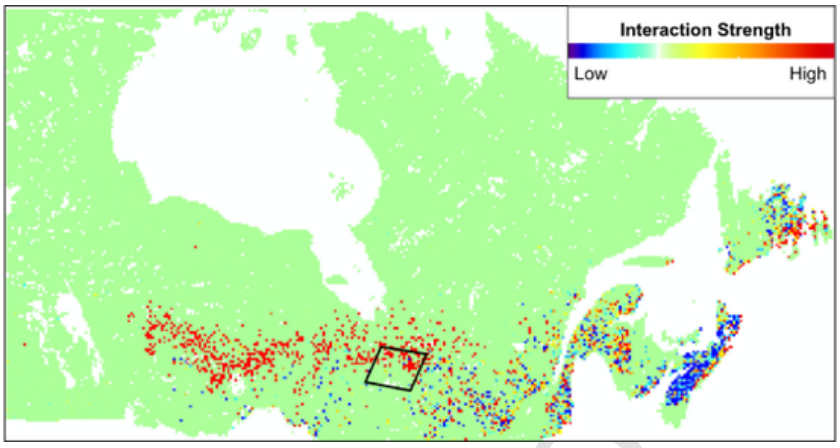

Fig. 10. Spatial distribution of interaction strength across Eastern Canada in terms of increases in burned area with eastern spruce budworm (ESBW) relative to control.

have physical implications, given that regions of dense fir will eventually experience defoliation over longer timescales and that the regeneration rates of host foliage may play an important role in return interval length, with additional sensitivity to mortality rates of past outbreaks. Thus, the spatial and temporal patterns of ESBW outbreak may be driven by specific aspects of the ecophysiology of balsam fir. Additionally, we found that mortality driven by ESBW defoliation enhanced burnt area, though by a small amount when averaged over space and time. Our study used climate data from the last century calibrated with aerial sketch maps to replicate patterns of the past. However, spatiotemporal patterns of outbreak and interactions with fire are likely to shift due to climate change, with potentially important contributions from shifts in host tree density.

Code and data availability

Code and data for this study are available at 10.5281/zenodo.6941561.

Uncited references

De Grandpré et al. (2019), , , Environment Canada: National Climate Data and Information Archive (2017), , , , , Pureswaran et al. (2019), , , .

CRediT authorship contribution statement

Hiromitsu Sato : Conceptualization, Methodology, Software, Validation, Writing – original draft, Formal analysis, Visualization, Writing – review & editing, Project administration. **Emeline Chaste :** Conceptualization, Software, Resources, Writing – review & editing. **Martin P. Girardin :** Conceptualization, Writing – review & editing, Software, Methodology, Resources, Project administration. **Jed O. Kaplan :** Writing – review & editing, Software, Methodology, Conceptualization. **Christelle Hély :** Conceptualization, Writing – review & editing. **Jean-Noel Candau :** Writing – review & editing, Software, Methodology. **Stephen J. Mayor :** Conceptualization, Writing – original draft, Writing – review & editing, Project administration.

Declaration of Competing Interest

The authors declare that they have no known competing financial interests or personal relationships that could have appeared to influence the work reported in this paper.

Data availability

Links in manuscript.

Acknowledgments

We would like to give thanks to Marc Oullette, Jemmett Kirk and Clara Risk for help with development and analysis of our project. Funding for this work was provided by the Ontario Ministry of Natural Resources and Forestry's Climate Change Program and the Canadian Forest Service. We thank Melanie Desrochers and Xiao Jing Guo for their help with mapping and computation for this project. We also thank Daniel Stubbs from Calcul Québec and Compute Canada for helping with the Fortran language and server space facilities for running LPJ-LMfire.

Supplementary materials

Supplementary material associated with this article can be found, in the online version, at doi:10.1016/j.ecolmodel.2023.110412.

References

Akalusi, M.E., Bourque, C.P.A., 2021. Physiological and morphological variation in balsam fir provenances growing in new brunswick, Canada. Forests 12 (2), 186.
Bachelet, D., Ferschweiler, K., Sheehan, T.J., Sleeter, B.M., Zhu, Z., 2018. Translating MC2 DGVM results into ecosystem services for climate change mitigation and adaptation. Climate 6 (1), 1.
Belyea, R.M., 1952. Death and deterioration of balsam fir weakened by spruce budworm defoliation in Ontario. Can. Entomol. 84 (11), 325–335.
Blais, J.R., 1981. Mortality of balsam fir and white spruce following a spruce budworm outbreak in the Ottawa river watershed in Quebec. Can. J. For. Res. 11 (3), 620–629.
Blais, J.R., 1983. Trends in the frequency, extent, and severity of spruce budworm outbreaks in eastern Canada. Can. J. For. Res. 13 (4), 539–547.
Bouchard, M., Régnière, J., Therrien, P., 2018. Bottom-up factors contribute to large-scale synchrony in spruce budworm populations. Can. J. For. Res. 48 (3), 277–284.
Boulanger, Y., Arseneault, D., 2004. Spruce budworm outbreaks in eastern Quebec over the last 450 years. Can. J. For. Res. 34 (5), 1035–1043.
Boulanger, Y., Arseneault, D., Morin, H., Jardon, Y., Bertrand, P., Dagneau, C., 2012. Dendrochronological reconstruction of spruce budworm (Choristoneura fumiferana) outbreaks in southern Quebec for the last 400 years. Can. J. For. Res. 42 (7), 1264–1276.
Candau, J.N., Fleming, R.A., Hopkin, A., 1998. Spatiotemporal patterns of large-scale defoliation caused by the spruce budworm in Ontario since 1941. Can. J. For. Res. 28 (11), 1733–1741.
Candau, J.N., Fleming, R.A., 2005. Landscape-scale spatial distribution of spruce budworm defoliation in relation to bioclimatic conditions. Can. J. For. Res. 35 (9), 2218–2232.
Candau, J.N., Fleming, R.A., 2011. Forecasting the response of spruce budworm defoliation to climate change in Ontario. Can. J. For. Res. 41 (10), 1948–1960.
Candau, J.N., Fleming, R.A., Wang, X., 2018. Ecoregional patterns of spruce budworm—wildfire interactions in central Canada's Forests. Forests 9 (3), 137.
Canelles, Q., Aquilué, N., James, P.M., Lawler, J., Brotons, L., 2021. Global review on

interactions between insect pests and other forest disturbances. Landsc. Ecol. 1–28.
Chaste, E., Girardin, M.P., Kaplan, J.O., Portier, J., Bergeron, Y., Hély, C., 2018. The pyrogeography of eastern boreal Canada from 1901 to 2012 simulated with the LPJ-LMfire model. Biogeosciences 15 (5), 1273–1292.
Chaste, E., Girardin, M.P., Kaplan, J.O., Bergeron, Y., Hély, C., 2019. Increases in heat-induced tree mortality could drive reductions of biomass resources in Canada's managed boreal forest. Landsc. Ecol. 34 (2), 403–426.
Chen, C., Weiskittel, A., Bataineh, M., Maclean, D.A., 2017. Even low levels of spruce budworm defoliation affect mortality and ingrowth but net growth is more driven by competition. Can. J. Forest Res. 47, 1546–1556. https://doi.org/10.1139/cjfr-201.
Coogan, S.C., Daniels, L.D., Boychuk, D., Burton, P.J., Flannigan, M.D., Gauthier, S., Wotton, B.M., 2021. Fifty years of wildland fire science in Canada. Can. J. For. Res. 51 (2), 283–302.
Crawford, H. S., Jennings, D. T., 1989. Predation by birds on spruce budworm Choristoneura fumiferana: functional, numerical, and total responses. Ecology 70 (1), 152–163.
Crawford, H. S., Titterington, R. W., Jennings, D. T., 1983. Bird predation and spruce budworm populations. Journal of Forestry 81 (7), 433–478.
De Grandpré, L., Kneeshaw, D.D., Perigon, S., Boucher, D., Marchand, M., Pureswaran, D., Girardin, M.P., 2019a. Adverse climatic periods precede and amplify defoliator-induced tree mortality in eastern boreal North America. J. Ecol. 107 (1), 452–467.
De Grandpré, M.P., Kneeshaw, D., Perigon, S., Boucher, D., Marchand, M., Pureswaran, D., Girardin, M.P., 2019b. Adverse climatic periods precede and amplify defoliator-induced tree mortality in eastern boreal North America. J. Ecol. 107, 452–467. https://doi.org/10.1111/1365-2745.13012.
Dymond, C.C., Neilson, E.T., Stinson, G., Porter, K., MacLean, D.A., Gray, D.R., Kurz, W.A., 2010. Future spruce budworm outbreak may create a carbon source in eastern Canadian forests. Ecosystems 13 (6), 917–931.
Environment Canada: National Climate Data and Information Archive. Available at climate.weatheroffice.gc.ca/, available from: http://climate.weatheroffice.gc.ca/(last access: 27 February 2017), 2013.
Fleming, R.A., Candau, J.N., McAlpine, R., 2002. Landscape-scale analysis of interactions between insect defoliation and forest fire in central Canada. Clim. Change 55, 251–272.
Girard, F., Payette, S., Gagnon, R., 2008. Rapid expansion of lichen woodlands within the closed-crown boreal forest zone over the last 50 years caused by stand disturbances in eastern Canada. J. Biogeogr. 35 (3), 529–537.
Girardin, M.P., Hogg, E.H., Bernier, P.Y., Kurz, W.A., Guo, X.J., Cyr, G., 2016. Negative impacts of high temperatures on growth of black spruce forests intensify with the anticipated climate warming. Glob Change Biol. 22 (2), 627–643.
Gray, D.R., MacKinnon, W.E., 2006. Outbreak patterns of the spruce budworm and their impacts in Canada. For. Chron. 82 (4), 550–561.
Gray, D.R., 2013. The influence of forest composition and climate on outbreak characteristics of the spruce budworm in eastern Canada. Can. J. For. Res. 43 (12), 1181–1195.
Hall, J.P., Moody, B.H., 1994. Forest Depletions Caused By Insects and Diseases In Canada, 1982-1987. Forest Insect and Disease Survey. Canadian Forest Service, Natural Resources Canada.
Han, E.N., Bauce, E., 1995. Non-freeze survival of spruce budworm larvae, Choristoneura fumiferana, at sub-zero temperatures during diapause. Entomol. Exp. Appl. 75 (1), 67–74.
Han, E.N., Bauce, E., Trempe-Bertrand, F., 2000. Development of the first-instar spruce budworm (Lepidoptera: tortricidae). Ann. Entomol. Soc. Am. 93 (3), 536–540.
Hantson, S., Arneth, A., Harrison, S.P., Kelley, D.I., Prentice, I.C., Rabin, S.S., Yue, C., 2016. The status and challenge of global fire modelling. Biogeosciences 13 (11), 3359–3375.
Hantson, S., Kelley, D.I., Arneth, A., Harrison, S.P., Archibald, S., Bachelet, D., Yue, C., 2020. Quantitative Assessment of Fire And Vegetation Properties In Simulations With Fire-Enabled Vegetation Models From The Fire Model Intercomparison Project., 13. Geoscientific Model Development, pp. 3299–3318.
IPCC, 2014: Climate change 2014: synthesis report. contribution of working groups I, II and III to the fifth assessment report of the intergovernmental panel on climate change [Core writing team, R.K. Pachauri and L.A. Meyer (eds.)]. IPCC, Geneva, Switzerland, 151 pp
James, P.M., Fortin, M.J., Sturtevant, B.R., Fall, A., Kneeshaw, D., 2011. Modelling spatial interactions among fire, spruce budworm, and logging in the boreal forest. Ecosystems 14 (1), 60–75.
James, P.M., Robert, L.E., Wotton, B.M., Martell, D.L., Fleming, R.A., 2017. Lagged cumulative spruce budworm defoliation affects the risk of fire ignition in Ontario, Canada. Ecol. Appl. 27 (2), 532–544.
Johns, R.C., Bowden, J.J., Carleton, D.R., Cooke, B.J., Edwards, S., Emilson, E.J., Stastny, M., 2019. A conceptual framework for the spruce budworm early intervention strategy: can outbreaks be stopped? Forests 10 (10), 910.
Kautz, M., Meddens, A.J., Hall, R.J., Arneth, A., 2017. Biotic disturbances in Northern Hemisphere forests–a synthesis of recent data, uncertainties and implications for forest monitoring and modelling. Global Ecol. Biogeogr. 26 (5), 533–552.
Keeling, R.F., Piper, S.C., Bollenbacher, A.F., Walker, J.S., 2009. Atmospheric CO2 Records from Sites in the SIO Air Sampling Network, in: Trends: A Compendium of Data on Global Change, Carbon Dioxide Information Analysis Center. Oak Ridge National LaboratoryUS Department of Energy, Oak Ridge, TN, USA. https://doi.org/10.3334/CDIAC/atg.035.
Koch, A., Kaplan, J.O., 2022. Tropical forest restoration under future climate change. Nat. Clim. Change 12 (3), 279–283.
Koller, C.N., Leonard, D.E., 1981. Comparison of energy budgets for spruce budworm Choristoneura fumiferana (Clemens) on balsam fir and white spruce. Oecologia 49 (1), 14–20.
Kurz, W.A., Stinson, G., Rampley, G.J., Dymond, C.C., Neilson, E.T., 2008. Risk of natural disturbances makes future contribution of Canada's forests to the global carbon cycle highly uncertain. Proc. Natl. Acad. Sci. 105 (5), 1551–1555.
Landry, J.S., Price, D.T., Ramankutty, N., Parrott, L., Matthews, H.D., 2016. Implementation of a Marauding Insect Module (MIM, version 1.0) in the Integrated BIosphere Simulator (IBIS, version 2.6 b4) Dynamic Vegetation–Land Surface Model, 9. Geoscientific Model Development, pp. 1243–1261.
Lavoie, J., Montoro Girona, M., Grosbois, G., Morin, H., 2021. Does the type of silvicultural practice influence spruce budworm defoliation of seedlings? Ecosphere 12 (4), e03506.
Li, F., Zeng, X.D., Levis, S., 2012. A process-based fire parameterization of intermediate complexity in a dynamic global vegetation model. Biogeosciences 9 (7), 2761–2780.
Liu, Z., Peng, C., De Grandpré, L., Candau, J.N., Work, T., Huang, C., Kneeshaw, D., 2019. Simulation and analysis of the effect of a spruce budworm outbreak on carbon dynamics in boreal forests of Québec. Ecosystems 22 (8), 1838–1851.
Lynch, H.J., Moorcroft, P.R., 2008. A spatiotemporal Ripley's K-function to analyze interactions between spruce budworm and fire in British Columbia, Canada. Can. J. For. Res. 38 (12), 3112–3119.
MacLean, D.A., 1980. Vulnerability of fir-spruce stands during uncontrolled spruce budworm outbreaks: a review and discussion. For. Chron. 56 (5), 213–221.
MacLean, D.A., 2019. Protection strategy against spruce budworm. Forests 10 (12), 1137.
Maréchaux, I., Langerwisch, F., Huth, A., Bugmann, H., Morin, X., Reyer, C.P., Bohn, F.J., 2021. Tackling unresolved questions in forest ecology: the past and future role of simulation models. Ecol. Evol. 11 (9), 3746–3770.
McCullough, D.G., Werner, R.A., Neumann, D., 1998. Fire and insects in northern and boreal forest ecosystems of North America. Annu. Rev. Entomol. 43 (1), 107–127.
Meigs, G.W., Zald, H.S., Campbell, J.L., Keeton, W.S., Kennedy, R.E., 2016. Do insect outbreaks reduce the severity of subsequent forest fires? Environ. Res. Lett. 11 (4), 045008.
Miller, C.A., 1975. Spruce budworm: how it lives and what it does. For. Chron. 51 (4), 136–138.
Miller, A., Rusnock, P., 1993. The rise and fall of the silvicultural hypothesis in spruce budworm (Choristoneura fumiferana) management in eastern Canada. For. Ecol. Manage. 61 (1–2), 171–189.
Morris, R.F., 1963. The dynamics of epidemic spruce budworm populations. Mem. Entomol. Soc. Can. 95 (S31), 1–12.
Morris, R.F., 1963b. The development of predictive equations for the spruce budworm based on key-factor analysis. Mem. Entomol. Soc. Can. 95 (S31), 116–129.
Navarro, L., Harvey, A.É., Ali, A., Bergeron, Y., Morin, H., 2018. A Holocene landscape dynamic multiproxy reconstruction: how do interactions between fire and insect outbreaks shape an ecosystem over long time scales? PLOS One 13 (10), e0204316.
Parisien, M.A., Barber, Q.E., Hirsch, K.G., Stockdale, C.A., Erni, S., Wang, X., Parks, S.A., 2020. Fire deficit increases wildfire risk for many communities in the Canadian boreal forest. Nat. Commun. 11 (1), 1–9.
Pavlick, R., Drewry, D.T., Bohn, K., Reu, B., Kleidon, A., 2013. The jena diversity-dynamic global vegetation model (JeDi-DGVM): a diverse approach to representing terrestrial biogeography and biogeochemistry based on plant functional trade-offs. Biogeosciences 10 (6), 4137–4177.
Pfeiffer, M., Spessa, A., Kaplan, J.O., 2013. A Model For Global Biomass Burning In Preindustrial Time: LPJ-LMfire (v1. 0), 6. Geoscientific Model Development, pp. 643–685.
Pureswaran, D.S., Johns, R., Heard, S.B., Quiring, D., 2016. Paradigms in eastern spruce budworm (Lepidoptera: tortricidae) population ecology: a century of debate. Environ. Entomol. 45 (6), 1333–1342.
Pureswaran, D.S., Neau, M., Marchand, M., De Grandpré, L., Kneeshaw, D., 2019. Phenological synchrony between eastern spruce budworm and its host trees increases with warmer temperatures in the boreal forest. Ecol. Evol. 9 (1), 576–586.
Pureswaran, D. S., Roques, A., Battisti, A., 2018. Forest insects and climate change. Current Forestry Reports 4, 35–50.
Quillet, A., Peng, C., Garneau, M., 2010. Toward dynamic global vegetation models for simulating vegetation–climate interactions and feedbacks: recent developments, limitations, and future challenges. Environ. Rev. 18, 333–353. . NA.
Rauchfuss, J., Ziegler, S.S., 2011. The geography of spruce budworm in eastern North America. Geogr. Compass 5 (8), 564–580.
Régnière, J., 1982. A process-oriented model of spruce budworm phenology (Lepidoptera: tortricidae). Can. Entomol. 114 (9), 811–825.
Régnière, J., 1983. An oviposition model for the spruce budworm, Choristoneura fumiferana (Lepidoptera: tortricidae). Can. Entomol. 115 (10), 1371–1382.
Régnière, J., 1987. Temperature-dependent development of eggs and larvae of Choristoneura fumiferana (Clem.)(Lepidoptera: tortricidae) and simulation of its seasonal history. Can. Entomol. 119 (7–8), 717–728.
Régnière, J., You, M., 1991. A simulation model of spruce budworm (Lepidoptera: tortricidae) feeding on balsam fir and white spruce. Ecol. Modell. 54 (3–4), 277–297.
Régnière, J., Seehausen, M. L., Martel, V., 2020. Modeling climatic influences on three parasitoids of low-density spruce budworm populations. Part 1: Tranosema rostrale (Hymenoptera: Ichneumonidae). Forests 11 (8), 846.
Régnière, J., St-Amant, R., Duval, P., 2012. Predicting insect distributions under climate change from physiological responses: spruce budworm as an example. Biol. Invasions 14 (8), 1571–1586.
Régnière, J., Nealis, V.G., 2019. Influence of temperature on historic and future population fitness of the western spruce budworm, Choristoneura occidentalis. Int. J. Pest Manag. 65 (3), 228–243.
Régnière, J., Cooke, B.J., Béchard, A., Dupont, A., Therrien, P., 2019. Dynamics and management of rising outbreak spruce budworm populations. Forests 10 (9), 748.
Robert, L.E., Kneeshaw, D., Sturtevant, B.R., 2012. Effects of forest management legacies on spruce budworm (Choristoneura fumiferana) outbreaks. Can. J. For. Res. 42 (3),

463–475.
Rothermel, R.C., 1972. A mathematical model for predicting fire spread in wildland fuels. In: Intermountain Forest & Range Experiment Station, 115. US Department of Agriculture, Forest Service.
Royama, T., MacKinnon, W.E., Kettela, E.G., Carter, N.E., Hartling, L.K., 2005. Analysis of spruce budworm outbreak cycles in New Brunswick, Canada, since 1952. Ecology 86 (5), 1212–1224.
Sato, H., Kelley, D.I., Mayor, S.J., Martin Calvo, M., Cowling, S.A., Prentice, I.C., 2021. Dry corridors opened by fire and low CO2 in Amazonian rainforest during the last glacial maximum. Nat. Geosci. 14 (8), 578–585.
Sitch, S., Smith, B., Prentice, I.C., Arneth, A., Bondeau, A., Cramer, W., Venevsky, S., 2003. Evaluation of ecosystem dynamics, plant geography and terrestrial carbon cycling in the LPJ dynamic global vegetation model. Glob Change Biol. 9 (2), 161–185.
Snell, R.S., 2014. Simulating long-distance seed dispersal in a dynamic vegetation model. Global Ecol. Biogeogr. 23 (1), 89–98.
Sonia, S., Morin, H., Krause, C., 2011. Long-term spruce budworm outbreak dynamics reconstructed from subfossil trees. J. Quat. Sci. 26 (7), 734–738.
Stein, U., Alpert, P.I.N.H.A.S, 1993. Factor separation in numerical simulations. J. Atmos. Sci. 50 (14), 2107–2115.
Stocks, B.J., Walker, J.D., 1973. Climatic Conditions Before and During Four Significant Forest Fire Situations in Ontario. Ontario Region Forest Research Laboratory.
Stocks, B.J., 1987. Fire potential in the spruce budworm-damaged forests of Ontario. For. Chron. 63 (1), 8–14.
Sturtevant, B.R., Miranda, B.R., Shinneman, D.J., Gustafson, E.J., Wolter, P.T., 2012. Comparing modern and presettlement forest dynamics of a subboreal wilderness: does spruce budworm enhance fire risk? Ecol. Appl. 22 (4), 1278–1296.
Tadaki, Y., 1966. Some discussions on the leaf biomass of forest stands and trees. Bull. Gov. For. Exp. Sta. 184, 135–161.
Temesgen, H., Weiskittel, A.R., 2006. Leaf mass per area relationships across light gradients in hybrid spruce crowns. Trees 20 (4), 522–530.
Thonicke, K., Venevsky, S., Sitch, S., Cramer, W., 2001. The role of fire disturbance for global vegetation dynamics: coupling fire into a Dynamic Global Vegetation Model. Global Ecol. Biogeogr. 10 (6), 661–677.
Thonicke, K., Spessa, A., Prentice, I.C., Harrison, S.P., Dong, L., Carmona-Moreno, C., 2010. The influence of vegetation, fire spread and fire behaviour on biomass burning and trace gas emissions: results from a process-based model. Biogeosciences 7 (6), 1991–2011.
Wania, R., Ross, I., Prentice, I.C., 2010. Implementation And Evaluation Of A New Methane Model Within A Dynamic Global Vegetation Model: lPJ-WHyMe v1. 3.1 3 (2), 565–584.
Watt, G.A., Stocks, B.J., Fleming, R.A., Smith, S.M., 2020. Stand breakdown and surface fuel accumulation due to spruce budworm (Choristoneura fumiferana) defoliation in the boreal mixedwood forest of central Canada. Can. J. For. Res. 50 (6), 533–541.
Venier, L. A., & Holmes, S. B. (2010). A review of the interaction between forest birds and eastern spruce budworm. *Environmental Reviews*, *18*(NA), 191-207.